

Long-Tailed Classification Based on Coarse-Grained Leading Forest and Multi-Center Loss

Jinye Yang¹, Ji Xu^{1*}

¹ State Key Laboratory of Public Big Data, Guizhou University, Guiyang, China
yjj@yer.xyz, jixu@gzu.edu.cn

Abstract—Long-tailed(LT) classification is an unavoidable and challenging problem in the real world. Most of the existing long-tailed classification methods focus only on solving the inter-class imbalance in which there are more samples in the head class than in the tail class, while ignoring the intra-class imbalance in which the number of samples of the head attribute within the same class is much larger than the number of samples of the tail attribute. The deviation in the model is caused by both of these factors, and due to the fact that attributes are implicit in most datasets and the combination of attributes is very complex, the intra-class imbalance is more difficult to handle. For this purpose, we proposed a long-tailed classification framework, known as COGNISANCE, which is founded on Coarse-Grained Leading Forest (CLF) and Multi-Center Loss (MCL), aiming to build a multi-granularity joint solution model by means of invariant feature learning. In this method, we designed an unsupervised learning method, i.e., CLF, to better characterize the distribution of attributes within a class. Depending on the distribution of attributes, we can flexibly construct sampling strategies suitable for different environments. In addition, we introduce a new metric learning loss, i.e., MCL, which aims to gradually eliminate confusing attributes during the feature learning process. More importantly, this approach does not depend on a specific model structure and can be integrated with existing LT methods as an independent component. We have conducted extensive experiments and our approach has state-of-the-art performance in both existing benchmarks ImageNet-GLT and MSCOCO-GLT, and can improve the performance of existing LT methods. Our codes are available on GitHub: <https://github.com/jinyery/cognisance>

Index Terms—Imbalanced learning, long-tailed learning, invariant feature learning.

I. INTRODUCTION

IN real-world applications, training samples typically exhibit a long-tailed distribution, especially for large-scale datasets [1], [2]. Long-tailed distribution means that a small number of head categories contain a large number of samples, while the majority of tail categories have a relatively limited number of samples. This imbalance can lead to traditional classification algorithms preferring to handle head categories and performing poorly when dealing with tail categories. Solving the problem of long-tailed classification is crucial as tail categories may contain important information such as rare diseases, critical events, or characteristics of minority groups [3], [4], [5], [6]. In order to effectively address this challenge, researchers have proposed various methods. However, what this article wants to emphasize is that the long-tailed distribution problem that truly troubles the industry is not all the inter-class long-tailed problem which is currently the most studied.

What truly hinders the further implementation of machine learning methods in the industry is the intra-class long-tailed problem, such as when it comes to the long-tailed distribution in unmanned vehicle training data, the weather distribution, day and night distribution [7], etc., are not the targets predicted by the model. Therefore, the long-tailed here is not among classes, but among attributes, where the attribute represents all the factors that cause intra-class changes, including object-level attributes (such as the specific vehicle model, brand, color, etc.) and image-level attributes (such as lighting, climate conditions, etc.), this emerging task is named **Generalized Long-Tailed Classification (GLT)** [8].

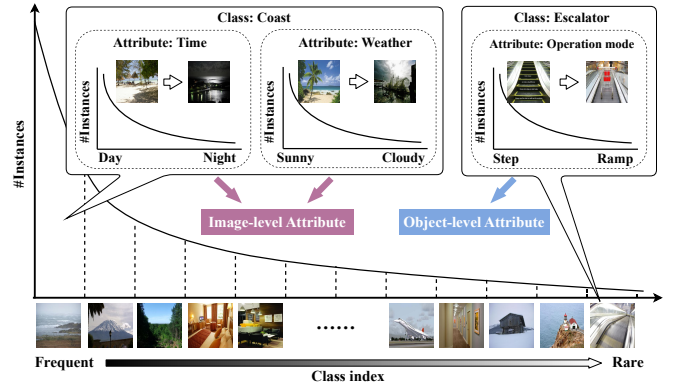


Fig. 1. Inter-class long-tailed distribution and intra-class long-tailed distribution.

In Fig. 1, it is evident that there is a significant difference in the number of samples among different categories, especially for the head class such as “Coast”, which has a much larger number of samples than the tail class such as “Escalator”. However, even within a category, there is a significant difference in the number of samples corresponding to different attributes. For example, in the category “Coast”, the number of samples during the day is much greater than that at night, and the number of samples on sunny days is also much greater than that on cloudy days. The imbalance in sample size among attributes within an category is fundamentally more difficult to avoid than the former, as shown in Fig. 2, this imbalance in attributes undermines the performance of the model in two ways [8]: I) Firstly, it weakens the accuracy of images with tail attributes. For example, black swans are more likely to be misclassified than white swans in the category “Swan”, even though they both belong to the same category. II) It leads

to some attributes being mistakenly associated with certain categories, e.g. the attribute “White” may be falsely correlated with “Swan”. Therefore, when “White” appears in images of other birds (e.g., “Cock”), there is a high risk that the sample will be misclassified as a “Swan”.



Fig. 2. Spurious correlation of the “White” attribute with the “Swan” category.

Current research mostly focuses on solving the inter-class long-tailed problem, where resampling [9], [10] or loss reweighting [11], [12] methods are often used when dealing with imbalanced data, aiming to rebalance the training process. However, most of these methods sacrifice the performance of the head class to improve the performance of the tail class, which is like playing a performance seesaw, making it difficult to fundamentally improve the performance of all classes. In addition, some methods believe that data imbalance does not affect feature learning, so the training of the model is divided into two stages through decoupling feature learning and classifier learning [13], [14]. However, this adjustment is only a trade-off between accuracy and precision [8], [15], and the confusion areas of similar attributes in the feature space learned by the model do not change. As mentioned earlier in this paper, it is precisely the long-tailed between attributes within a category that leads to spurious correlations between the head attributes of certain categories and that category. This means that these attributes correspond to the spurious features (i.e., a confusing region in the feature space) of the category. The method proposed in this paper aims to eliminate the confusing region based on the invariant feature learning, which ultimately achieves the goal of improving the model’s precision and accuracy at the same time [16], [17], [18].

In the framework proposed in this paper, inter-class and intra-class long-tailed problems are handled simultaneously by constructing different environments, in which we design a new sampling method **Coarse-Grained Leading Forest (CLF)**, which is based on unsupervised learning that can characterize the attribute distributions within a class and guide the data sampling in different environments during the training process. In the experimental setup of this paper, two environments are constructed, one of which is the original environment without special treatment, and the other environment in which the distributions of categories and attributes tend to be balanced. Finally, in order to gradually eliminate confusing pseudo-features during the training process, we design a new metric learning loss, **Multi-Center Loss (MCL)**, which is inspired by [8] and [19], extends the center loss to its Invariant Risk Minimization (IRM) version, and further improves the robustness of the model compared to the previous two, giving

the model the ability to learn invariant features. In addition, this method is not coupled with a specific backbone model or loss function, and can be seamlessly integrated into other LT methods for performance enhancement on top of the original.

Our contributions can be summarized as follows:

- We designed a novel unsupervised learning-based sampling scheme to guide the sampling of different environments in the IRM process, while dealing with the inter-class long-tail problem as well as the intra-class long-tailed problem among attributes, which is often neglected in traditional methods.
- We combined the idea of invariant feature learning to design a new metric learning loss, which can enable the model to gradually remove the influence of pseudo-features during the training process, further improving the robustness of the model and taking into account the precision and accuracy of the prediction.
- We conducted extensive experiments on two existing benchmarks, ImageNet-GLT and MSCOCO-GLT, to validate the effectiveness of this framework while improving the performance of all popular LT lineups.

II. RELATED WORK

A. Long-Tailed Classification

The key challenge of long-tailed classification is to effectively deal with the imbalance of data distribution to ensure that excellent classification performance can be achieved both between the head and the tail. Current treatments for long-tailed classification can be broadly categorized into three groups [1]: 1) Class Re-balancing, which is the mainstream paradigm in long-tailed learning, aims to enhance the influence of tail samples on the model by means of re-sampling [20], [10], [21], [22], re-weighting [23], [24], [25], [26], [27] or logit adjustment [28] during the model training process, and some of these methods [13], [14] consider that the unbalanced samples do not affect the learning of the features, and thus divide feature learning and classifier learning into two phases, and perform operations such as resampling only in the classifier learning phase. 2) Information Augmentation, information augmentation based approaches seek to introduce additional information in model training in order to improve model performance in long-tailed learning. There are two approaches in this method type: migration learning [29], [30], [31] and data augmentation [32], [33], [34]. 3) Module Improvement, in addition to class rebalancing and information augmentation, researchers have explored ways to improve network modules in long-tailed learning such as RIDE [35] and TADE [36], both of which deal with long-tail recognition independent of test distribution by introducing integrated learning of multi-expert models in the network.

In addition, a recent study proposed the concept of Generalized Long-Tailed Classification (GLT) [8], which first pointed out the problem of long-tailed of attributes within a class, which pointed out that the traditional long-tailed classification methods represent the classification model as $p(Y|X)$, i.e., predicting the label Y from the input image X , which can be further decomposed as $p(Y|X) \propto p(X|Y) \cdot p(Y)$, the

formula identifies the cause of class bias as $p(Y)$. However, the distribution of $p(X|Y)$ also changes in different domains, so the classification model is extended to the form of Equation 1 based on the Bayesian Theorem in this study.

$$p(Y = k|z_c, z_a) = \frac{p(z_c|Y = k)}{p(z_c)} \cdot \underbrace{\frac{p(z_a|Y = k, z_c)}{p(z_a|z_c)}}_{\text{attribute bias}} \cdot \underbrace{p(Y = k)}_{\text{class bias}}, \quad (1)$$

where z_c is the invariant present in the category, and the attribute-related variable z_a is the domain-specific knowledge in different distributions. Taking the mentioned “swan” as an example, the attribute “color” of “Swan” belongs to z_a , while the attributes of “Swan” such as feathers and shape belong to z_c , and it is worth noting that in practical applications the formula does not impose the untangling assumption, i.e., it does not assume that a perfect feature vector $z = [z_c; z_a]$ can be obtained, where z_a and z_c are separated.

B. Invariant Risk Minimization

IRM [17] was proposed by Arjovsky et al. in 2019, and its main goal is to build robust learning models that can have the same performance on different data distributions. In machine learning, we usually hope that the trained model can perform well on future data, which is called Risk Minimization. However, in practice, there may be distributional differences between the training data and the test data, known as Domain Shift, which causes the model to perform poorly on new domains. The core idea of IRM is to solve the domain adaptation problem by encouraging models to learn features that are invariant across data domains. This means that the model should focus on those shared features that are present in all data domains rather than overfitting a particular data distribution.

$$\begin{aligned} & \min_{\substack{\Phi: \mathcal{X} \rightarrow \mathcal{H} \\ w: \mathcal{H} \rightarrow \mathcal{Y}}} \sum_{e \in \varepsilon_{tr}} R^e(w \circ \Phi) \\ & \text{subject to } w \in \arg \min_{\bar{w}: \mathcal{H} \rightarrow \mathcal{Y}} R^e(\bar{w} \circ \Phi), \text{ for all } e \in \varepsilon_{tr} \end{aligned} \quad (2)$$

As shown in 2, where ε_{tr} represents all environments, \mathcal{X} , \mathcal{H} , and \mathcal{Y} represent inputs, feature representations, and prediction results, respectively, Φ and w are feature learner and classifier, respectively, and R^e denotes the risk under the environment e , the goal of IRM is to find a common solution that can perform stably on all environments, thus improving the model’s generalization ability.

C. Optimal Leading Forest

The CLF proposed in this paper starts with OLeaF [37], so we provide a brief introduction to its ideas and algorithms here. The concept of optimal leading forest originates from a clustering method based on density peak [38], and the two most critical factors in the construction of OLeaF are the density of the data points and the distance of the data points to their nearest neighbors with higher density. Let $I = \{1, 2, \dots, N\}$ be the index set of dataset \mathcal{X} , and $d_{i,j}$ represent the distance between data points x_i and x_j (any distance metric can be

used), and let $\rho_i = \sum_{j \in I \setminus \{i\}} \exp(-(d_{i,j}/d_c)^2)$ be the density of data point x_i , where d_c is the cut-off distance. If there exists $\xi_i = \operatorname{argmin}_j \{d_{i,j} | \rho_j > \rho_i\}$, then x_{ξ_i} is said to be the leading node of x_i . Based on this a partial order relation can be established, i.e., if there exists $\xi_i = \eta(x_i)$, then $x_i \prec x_{\xi_i}$, and connecting every x_i and x_{ξ_i} (for $r = \operatorname{argmax}_{1 \leq i \leq N} \{\rho_i\}$, then x_r is the root node) based on the partial order bias, a tree structure can be established and is known as the Leading Tree. And then let $\delta_i = d_{\xi_i, i}$, $\gamma_i = \rho_i \times \delta_i$, then the larger γ_i represents the higher potential of the data point x_i to be selected as the cluster center. Intuitively, if an object has a large x_i , it means it has a lot of close neighbors, and δ_i is large, it is far away from another data point with a large ρ_i value, so x_i has a good chance to become the center of the cluster, and the root node can be selected based on the ordering of γ_i . Then a Leading Tree will be partitioned in this way, and the resulting multiple Leading Tree will be called an Optimal Leading Forest (OLeaF).

III. THE PROPOSED COGNISANCE FRAMEWORK

In the previous introduction of GLT [8], attribute bias and class bias were introduced, and traditional LT methods tend to focus only on the latter, and the resampling, reweighting, etc. designed based on this tend to focus only on the distribution of classes. As a matter of fact, as the example given earlier, attribute bias not only impairs the model’s performance on tail attribute samples within a class, but also it is the spurious correlation between some head attributes with pseudo-features and certain classes that leads to the imbalance of the model’s performance among classes. Therefore, in order to improve the generalization ability of the model on data with different category distributions and different attribute distributions, this paper proposes a framework named COGNISANCE based on invariant feature learning, which firstly uses Coarse-Grained Leading Forest to construct different environments with different data distributions, and then under Multi-Center Loss, the model is allowed to learn invariant features in each data domain instead of overfitting a certain distribution to solve the multi-domain adaptation problem.

A. Coarse-Grained Leading Forest

In the concept of IRM [17], the construction of different environments is a prerequisite for training, and the challenge in this paper is to construct controllable environments with different attribute distributions. Environments with different category distributions are easy to construct because the labels of the categories are explicit in the dataset, while the attributes are implicit for most datasets, and even if the category imbalance is completely eliminated, its attribute imbalance still exists. At the same time, because of the nature that attributes can be continuously superimposed and combined, the boundaries of attributes are also complex, thus we design a sampling method based on unsupervised learning, which can portray the distribution of attributes within the same category and can control the granularity of the portraying of attributes according to the setting of hyperparameters.

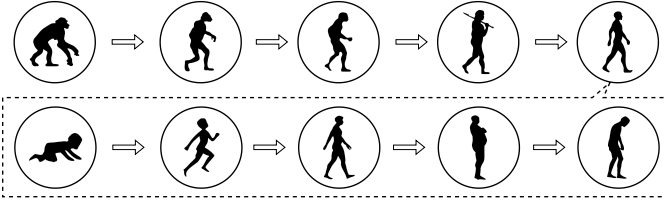


Fig. 3. Evolution of intra-class samples, the samples within the class have delicate transitions.

Our motivation is based on a reasonable assumption that the differences between samples within the same category are the result of the gradual separation and evolution of attributes. This is somewhat similar to a biological evolutionary tree, where the gap from the root node to the leaf nodes doesn't happen all at once, but is the result of constant evolution and branching, while the evolution is not only reflected at a coarse-grained level, but within the same category, the transition will be more subtle.

As shown in Fig. 3, even within the “human” category, the samples between different ages are clustered and transition gradually. Of course, in a manually collected dataset, not all changes within a class may be gradual, and if the differences among more granular groups within a class are too large, then the class cannot be portrayed by a single tree. In other words, when there is a common ancestor node, the samples within a class can be viewed as a whole with the characteristics of streaming transformation, but when the ancestor node is removed, the gap between two sub-branches will be too large, which should actually be portrayed with two or more trees instead of forcibly connected together. Based on the above analysis, we designed a new clustering algorithm Coarse-Grained Leading Forest in combination with the construction of OLeaF [37], and its construction process is shown in Algorithm 1. Firstly, the distance matrix between the sample points in the dataset X is computed using an arbitrary distance metric, and then the density of each sample point is computed, where the density of sample point i is computed as shown in Equation 3:

$$\rho_i = \sum_{j \in I \setminus \{i\} \setminus O_i} \exp\left(- (d_{i,j}/d_{max})^2\right), \quad (3)$$

where $I = \{1, 2, \dots, N\}$ is the index set of dataset X , O_i is the set of nodes whose distance from node i exceeds d_{max} , $d_{i,j}$ is the distance between node i and node j , and d_{max} is the cut-off distance. Next sort I in descending order according to the density value, denoted as S , i.e., S_i is the index of the data point with the i -th largest density value. The next step is to perform small-scale clustering on the points in S sequentially, which relies on the hyperparameter d_{min} , and if the data point S_i has not yet been merged into a coarse-grained node, then the data point S_i and the points within d_{min} distance from it are formed into a coarse-grained node, i.e.:

$$C_{mem} = \{S_i\} \cup K \setminus A, \quad S_i \notin A, \quad (4)$$

where C_{mem} are members of the newly generated coarse-grained node, S_i will be an agent node for that coarse-grained

node, K is the set of nodes that are within d_{min} from S_i , i.e., $K = \{j \mid j \in I, d_{S_i,j} < d_{min}\}$, and A is the set of visited nodes, i.e., the set of nodes that have already been merged into a particular coarse-grained node. Note that if S_i itself is already in A then it skips the creation of that new coarse-grained node and continues to process the next node in S . The

Algorithm 1: Construction of CLF

Input: All training samples X of a given category.

Output: A Coarse-Grained Leading Forest clf for a given category.

Parameter: d_{min} is the radius of the coarse-grained node, d_{max} is the cut-off distance.

```

1  $dist = \text{calculate\_distance}(X)$ ;
2  $density = \text{calculate\_density}(dist, d_{max})$ ;
3  $density\_argsort = \text{argsort}(density, \text{descend}=\text{True})$ ;
  // Record the index of samples that
  // have been visited
4  $accessed = \text{initial\_vector}(\text{length}(density), \text{False})$ ;
5 for  $i$  in  $\text{range}(\text{length}(density))$  do
6    $node\_idx = density\_argsort[i]$ ;
7   if  $accessed[node\_idx]$  then
8     continue;
9   end
  // Combine points that are within
  //  $d_{min}$  and have not been visited
  // into one coarse-grained node.
10   $c\_members = \text{where}(accessed == \text{False} \text{ and } dist[node\_idx] \leq d_{min})$ ;
11   $accessed[c\_members] = \text{True}$ ;
12   $coarse\_node = \text{CoarseNode}(\text{id}=\text{Autoincrement}, \text{agent}=node\_idx, \text{members}=c\_members)$ ;
  // A node becomes a root node if no
  // denser leading node can be found
  // within  $d_{max}$ .
13   $leader\_node = \text{find\_leader}(node\_idx, d_{max})$ ;
14  if  $leader\_node$  is not null then
15     $coarse\_node.leader = leader\_node$ ;
16  end
17  else
18     $clf.root.append(coarse\_node)$ ;
19  end
20 end
21 return  $clf$ ;

```

next step is to find the leading node of the newly constructed coarse-grained node. Here, the problem is transformed into finding the leading node of the agent node S_i of the coarse-grained node, denoted as l_i , and then the coarse-grained node where l_i is located is used as the leading node of the current coarse-grained node. The process of finding the leading node l_i of S_i can be referred to Equation 5, where O_{S_i} is the set of nodes whose distance from S_i exceeds d_{max} :

$$l_{S_i} = \underset{j}{\operatorname{argmin}} \{d_{S_i,j} \mid \rho_j > \rho_{S_i}, j \in I \setminus \{S_i\} \setminus O_{S_i}\}, \quad (5)$$

note that l_{S_i} may not exist, and when l_{S_i} is not found, the coarse-grained node where S_i is located automatically

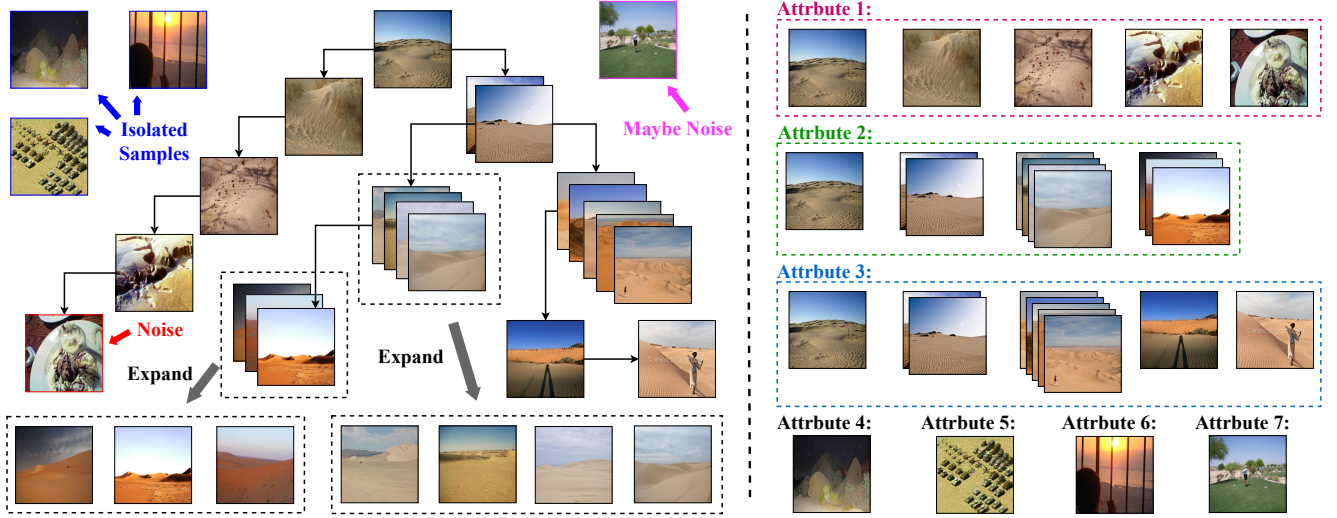


Fig. 4. The left is an example of CLF constructed for category “sand”, while the right is an example of attribute splitting using CLF. Each path from the root node to the leaf nodes can be considered as an attribute, and the samples within the coarse-grained nodes are extremely similar, requiring an appropriate reduction in sampling weights. In addition the samples within the red and pink boxes demonstrate the potential of this method for noisy recognition.

becomes a root in the whole coarse-grained leading forest. Also since the density of nodes in \mathcal{S} is decreasing, when l_{S_i} is found, it must have been processed and already merged into a coarse-grained node since l_{S_i} is denser.

B. Sampling based on CLF

By constructing the CLF we can simulate the portraying of attribute distributions within a category, and by adjusting the hyperparameters d_{min} and d_{max} , we can control the fineness of the portraying. Next, we can construct the environment of different attribute distributions based on CLF, as shown in Fig. 4, because each branch represents a new direction of attribute evolution, and we categorize all the data points on each path from the root node to the leaf nodes as members of a certain attribute branch.

When we obtain the samples of each attribute, we can refer to the idea of inter-class resampling [13] to resample on the attributes, as shown in Equation 6, when inter-class sampling is performed, j represents the class index, n_j represents the number of samples of class j , and C represents the total number of classes, where $q \in [0, 1]$, and inter-class balanced sampling is performed when $q = 0$.

$$p_j = \frac{n_j^q}{\sum_{i=1}^C n_i^q} \quad (6)$$

As shown in Algorithm 2, when sampling different attributes within a category, the idea is the same as inter-class sampling, only need to regard j as the attribute index, n_j as the number of samples of attribute j , and C as the total number of attributes. In addition, it should be noted that in intra-class sampling, unlike inter-class sampling, the same sample may have more than one attribute (e.g., the root node appears in all branches of the same tree, so it has all the attributes that this tree can represent), so the weight of such a sample point needs to be penalized to some extent. At the same time, due to the concept of coarse-grained node in our algorithm, as shown in

Fig. 4, the variance of the members in the coarse-grained nodes is extremely small, i.e., the representativeness of the sample decreases, and the value of the information provided decreases, so the sampling weight of the members in the coarse-grained nodes should be appropriately reduced. In this paper, we use the method where all members within a CoarseNode share the weight of that CoarseNode equally.

Taking the trunk tree in CLF in Fig. 4 as an example (ignoring isolated samples for demonstration purposes), we will provide a detailed introduction to attribute balanced sampling. Firstly, different attributes can be separated based on CLF, as shown in Fig. 4, each path from the root node to the leaf node can be considered as an attribute, which means that if you want to evenly sample the samples of each attribute, you only need to assign equal sampling weights to each attribute. Where for nodes that are repeated in multiple paths, we simply divide their sampling weight by the number of repetitions as a penalty. Take the example of calculating the weight of the root node, firstly since there are three attribute groups, so $weight = \frac{1}{3}$, and then the node’s weight in the three attribute groups are $\frac{1}{5}$, $\frac{1}{4}$, and $\frac{1}{5}$, so the root node’s sampling weights globally are $\frac{1}{15}$, $\frac{1}{12}$, and $\frac{1}{15}$, and summing up the three weights yields $weight = \frac{13}{60}$, and finally an appropriate penalty is to be applied, i.e., $weight = \frac{weight}{repetition} = \frac{13}{180}$. Furthermore, for a CoarseNode containing multiple samples, the penalty is similar, setting the sampling weight of each sample to $weight = CoarseNode.weight / CoarseNode.length$. Taking the second coarse-grained node in Attribute 2 as an example, the sampling weight of this node is $weight = (\frac{1}{3} \times \frac{1}{4} + \frac{1}{3} \times \frac{1}{5}) / 2 = \frac{3}{40}$, and the sampling weight of each sample in this coarse-grained node is $weight = \frac{3/40}{2} = \frac{3}{80}$.

C. Multi-Center Loss

In the previous step multiple training environments for invariant feature learning were constructed, and the next step is to train using the objective function of IRM [17], however,

Algorithm 2: Sampling according to CLF

Input: A Coarse-Grained Leading Forest *clf*, balance factor *q*

Output: The sampling probability of each sample within a certain category weights

```

// Initialize an array with 0 to
// record the sampling weights for
// each sample.
1 weights = initial_vector(default=0);
// Generate the path from the root
// node to the leaf node based on
// clf.
2 paths = generate_path(clf);
// Get the number of times each node
// appears in all paths.
3 repetitions = get_repetition(paths);
// Calculate the probability of each
// path being sampled based on q.
4 path_weight = get_path_weight(paths, q);
5 foreach path in paths do
    // CoarsedNodes in the same path
    // have the same sampling weight.
6 coarse_node_weight = path_weight / len(path);
7 foreach node in path do
    // All members within a
    // CoarsedNode share the
    // sampling weight of that node
    // equally.
8 small_node_weight = coarse_node_weight /
    len(node.members);
9 weights[node.members] +=
    small_node_weight;
10 end
11 end
// Apply some penalty to nodes that
// have appeared in more than one
// path.
12 weights / = repetitions;
13 return weights;

```

since the original IRM loss has convergence problems in realistic datasets, we designed a new goal Multi-Center Loss based on the idea of IRM and the center loss in IFL [8], which can be formulated as the following optimization problem:

$$\begin{aligned}
& \min_{\theta, \omega} \sum_{e \in \mathcal{E}} \sum_{i \in e} L_{cls}(f(x_i^e; \theta), y_i^e; \omega) \\
& \text{s.t. } \theta \in \arg \min_{\Theta} \sum_{e \in \mathcal{E}} \sum_{i \in e} \|f(x_i^e; \Theta) - C(x_i)\|_2,
\end{aligned} \quad (7)$$

where Θ and ω are the learnable parameters of the backbone and classifier, respectively, x_i^e and y_i^e are the i -th instance in environment e and its label, respectively, \mathcal{E} is all the training environments, $f(x_i^e; \theta)$ is the feature extracted by the backbone from x_i^e , $L_{cls}(f(x_i^e; \theta), y_i^e; \omega)$ is the classification loss under environment e (arbitrary loss function), and $C(x_i)$ is the center to which x_i^e belongs in all environments \mathcal{E} . Note

that the number of centers in each category $n_{c_{y_i}} \geq 1$, and the center to which x_i^e belongs depends on which tree in the CLF of that category x_i^e is located, i.e., $n_{c_{y_i}} = n_{t_{y_i}}$, where $n_{t_{y_i}}$ is the number of trees in the CLF constructed from all samples of that category, and the initial value of $C(x_i)$ is the value of the *agent* of the root node of the tree where x_i^e is located. The practical version of this optimization problem is shown in Equation 8, where $L_{IFL} = \|f(x_i^e; \theta) - C(x_i)\|_2$ is the constraint loss for invariant feature learning and α is the trade-off parameter:

$$\begin{aligned}
\min_{\theta, \omega} \sum_{e \in \mathcal{E}} \sum_{i \in e} L_{mc} &= \min_{\theta, \omega} \sum_{e \in \mathcal{E}} \sum_{i \in e} L_{cls} + \alpha \cdot L_{IFL} \\
&= \min_{\theta, \omega} \sum_{e \in \mathcal{E}} \sum_{i \in e} L_{cls}(f(x_i^e; \theta), y_i^e; \omega) \\
&\quad + \alpha \cdot \|f(x_i^e; \theta) - C(x_i)\|_2,
\end{aligned} \quad (8)$$

this loss is the IRM version of center loss, on the other hand, relative to the original version of center loss increases the robustness, as in the previous introduction of CLF, in some artificial datasets, even within the same category there may be a situation where the gap between the samples is extremely large, i.e., the number of trees in CLF is greater than 1, as shown in Fig. 5, in category “garage”, it can actually be divided into three categories: “Outside the garage”, “Inside the garage with car”, and “Inside the garage without car”, and the features of these three subclasses vary greatly. If only one center is used, making each category’s features gradually approach one center during the training process will actually damage the learning of features, and this is the starting point for using Multi-Center.

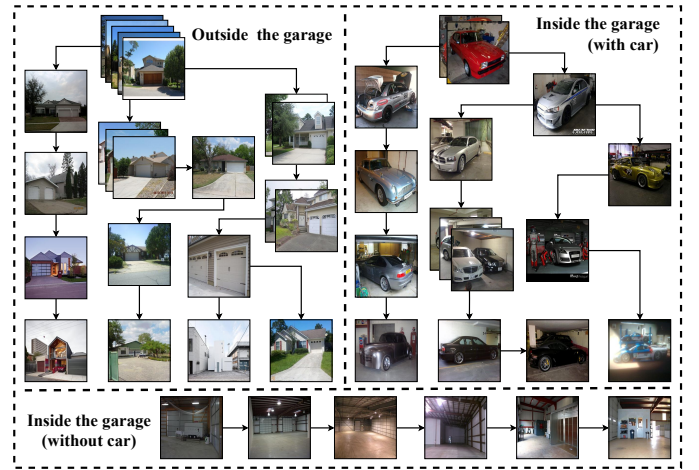


Fig. 5. Multiple trees in the CLF of category “garage” (only part of it is shown), there are multiple subclasses in the category “garage”, e.g., outside the garage, inside the garage (parked cars), and inside the garage (no parked cars), and there is a huge disparity among these subclasses.

D. Overall Framework

The overall framework of this scheme is shown in Fig. 6. Each environment has a pair of (q_{cls}, q_{attr}) , with the former being the balance factor for inter-class sampling and the latter being the balance factor for intra-class sampling. Different environments can be constructed through different (q_{cls}, q_{attr})

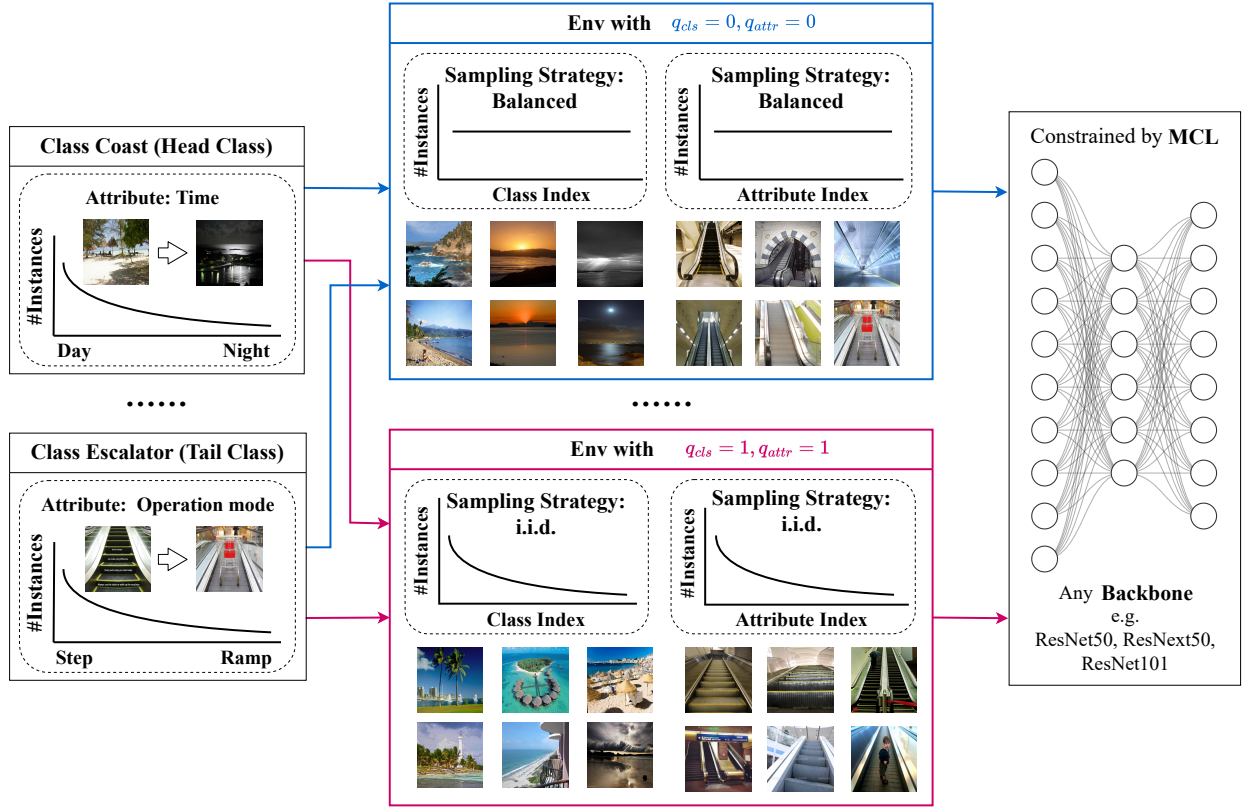


Fig. 6. Overall framework diagram, where different environments have different sampling strategies, where q_{cls} and q_{attr} are balancing factors for inter-class sampling and intra-class sampling, respectively.

pairs, and model parameters can be shared for training under the constraint of MCL. The portraying of attribute distribution during sampling is achieved through CLF, while the number of centers in MCL is determined by the number of trees in CLF of the corresponding category.

The algorithm process of the overall framework is shown in Algorithm 3, which is divided into two stages: firstly, since the initial features of the samples need to be used for clustering when constructing CLF, M -round normal sampling training is required to obtain an initial model with imperfect predictions; Next, the initial features are used to construct the CLF, and different environments are constructed through the CLF and different balance factor pairs. For example, in the experimental phase, this article sets up two environments with balance factor pairs of $(q_{cls}^{e1} = 1, q_{attr}^{e1} = 1)$ and $(q_{cls}^{e2} = 0, q_{attr}^{e2} = 0)$, where the former is a normal i.i.d. sampling environment and the latter is a balanced sampling environment for both categories and attributes. Then, the feature learner is continuously updated to further update the center in the CLF and MCL. Of course, the number of epoch steps for executing updates in the second stage can be adjusted, rather than being fixed to one update per epoch.

IV. EXPERIMENT

A. Evaluation Protocols

Before conducting the experiment, it is necessary to first introduce two new evaluation protocols: CLT Protocol and

Algorithm 3: The overall of the proposed COGNISANCE algorithm

Input: the original training set $\{(x, y)\}$; balance parameter pairs $\{(q_{cls}^e, q_{attr}^e)\}$ for different environments.

Output: backbone $f(\cdot; \theta)$, classifier $g(\cdot; w)$

```

1 Initialize: backbone  $f(\cdot; \theta)$ , classifier  $g(\cdot; w)$ ;
2 for  $M$  warm-up epochs do
3   // optimizing the model from cross-entropy
   classification loss;
4    $\theta, w \leftarrow \hat{\theta}, \hat{w} \in \arg \min_{\theta, w} L_{cls}(g(f(x; \theta); w), y)$ ;
5 end
6  $\{F_y\} = \text{ClfConstruct}(\{(x, y)\}, \theta, w)$ ;
7  $\{e_n\} = \text{EnvConstruct}(\{(q_{cls}^e, q_{attr}^e)\}, \{F_y\})$ ;
8 for  $N$  epochs do
9    $\{(x^e, y^e)\} = \text{DataLoader}(\{e_n\})$ ;
10   $\{C_y\} = \text{ReadCenters}(\{F_y\})$ ;
11   $\theta, w \leftarrow \hat{\theta}, \hat{w} \in \arg \min_{\theta, w} L_{cls}(g(f(x; \theta); w), y) +$ 
    $\alpha \cdot L_{mc}(f(x; \theta), \{C_y\})$ ;
12   $\{F_y\} = \text{ClfConstruct}(\{(x, y)\}, \theta, w)$ ;
13   $\{e_n\} = \text{EnvConstruct}(\{(q_{cls}^e, q_{attr}^e)\}, \{F_y\})$ ;
14 end

```

GLT Protocol, both of which were proposed in the first baseline of GLT [8]:

- **Class wise Long Tail (CLT) Protocol:** The samples in the training set follow a long-tailed distribution, which means that they are normally sampled from the LT dataset, while the samples in the test set are balanced by class. Note that the issue of attribute distribution is not considered in CLT, as the training and testing sets of CLT have the same attribute distribution and different class distributions, so the effectiveness of category long tail classification can be evaluated.
- **Generalized Long Tail (GLT) Protocol:** Compared with the former, the difference in attribute distribution is taken into account, that is, the attribute bias in Equation 1 is introduced. The training set in GLT is the same as that in CLT and conforms to the LT distribution, while the attribute distribution in the test set tends to be balanced. Since the train set and test set in GLT have different attribute distributions and different class distributions, it is possible to evaluate the model's ability to handle both inter-class long-tailed classification and intra-class long-tailed classification.

B. Datasets and Metrics

In total, we evaluated and compared the LT methods on two benchmarks, MSCOCO-GLT, and ImageNet-GLT, which are proposed in the first baseline of GLT [8].

ImageNet-GLT is a long-tailed subset of ImageNet [39], where the train set contains 113k samples of 1k classes, where the number of each class ranges from 570 to 4. The number of test set in both CLT and GLT protocols is 60k, and the test set are divided into three subsets according to the following class frequencies: $\#sample > 100$ for

$Many_C$, $100 \geq \#sample \geq 20$ for $Medium_C$, and $\#sample < 20$ for Few_C . Note that in constructing the test set for attribute balancing in this dataset, the images in each category were simply clustered into 6 groups using KMeans, and then 10 images were sampled for each group in each category.

MSCOCO-GLT is a long-tailed subset of MSCOCO-Attribute [40], a dataset explicitly labeled with 196 different attributes, where each object with multiple labels is cropped as a separate image. The train set contains 144k samples from 29 classes, where the number of each class ranges from 61k to 0.3k, and the number of test set is 5.8k in both the CLT and GLT protocols, and the test set are divided into three subsets according to the following category frequencies: $Index_C \leq 10$ for $Many_C$, $22 \geq Index_C \geq 10$ for $Medium_C$ and $Index_C > 22$ for Few_C , where $Index_C$ is the index of the category in ascending order.

Evaluation Metrics. In our experiments in this paper we use two metrics to evaluate the performance of the methods: 1) Accuracy: $\frac{\#CorrectPredictions}{\#AllSamples}$, which is the Top-1 Accuracy that has been used in traditional long-tailed methods; 2) Precision: $\frac{1}{\#class} \cdot \sum_{class} \frac{\#CorrectPredictions}{\#SamplesPredictedAsThisClass}$, the reason why this metric is introduced is to better reveal the precision-accuracy trade-off problem [8] that has not been paid attention to in traditional inter-class long-tailed methods.

C. Comparisons with LT Line-up

This scheme handles both the inter-class long-tailed problem and the intra-class long-tailed problem by eliminating the false correlation caused by attributes, and this scheme can be seamlessly combined with other LT methods. In the following comparison experiments we follow the classification of current long-tailed research in [1] and [8], and classify current long-

TABLE I
EVALUATION OF CLT AND GLT PROTOCOLS ON IMAGENET-GLT

| Protocols | | Class-Wise Long Tail (CLT) Protocol | | | | Generalized Long Tail (GLT) Protocol | | | |
|---|--------------------------|-------------------------------------|-----------------------------|---------------------|-----------------------------|--------------------------------------|-----------------------------|----------------------------|-----------------------------|
| $\langle \text{Accuracy} \mid \text{Precision} \rangle$ | | $Many_C$ | $Medium_C$ | Few_C | Overall | $Many_C$ | $Medium_C$ | Few_C | Overall |
| Re-balance | Baseline | 58.39 38.35 | 36 52.15 | 13.98 55.34 | 41.65 47.11 | 50.7 32.5 | 27.8 43.99 | 10.18 47.7 | 34.32 39.95 |
| | BBN | 62.66 43.45 | 44.36 55.44 | 14.66 57.57 | 47.22 50.96 | 53.37 36.45 | 34.97 46.81 | 10.73 46.08 | 38.7 42.56 |
| | BLSoftmax | 54.03 47.07 | 41.65 46.83 | 28.37 37.58 | 44.61 45.54 | 46.45 40.45 | 32.67 38.59 | 21.38 29.57 | 36.49 37.98 |
| | Logit-Adj | 53.3 49.05 | 43.49 44.12 | 31.86 35 | 45.67 44.72 | 45.43 41.75 | 34.2 35.9 | 24.58 27.78 | 37.25 37.02 |
| | GLTv1 | 62.51 42.32 | 38.69 57.23 | 17.41 65 | 45.03 52.43 | 54.4 36.23 | 30.18 49.61 | 12.64 55.47 | 37.24 45.14 |
| | * Baseline + COGNISANCE | 62.84 42.82 | 39.62 57.25 | 18.61 61.55 | 45.76 52.12 | 54.53 36.47 | 31.3 49.99 | 13.8 58.27 | 37.97 45.82 |
| | * BLSoftmax + COGNISANCE | 58.37 53.88 | 44.98 51.97 | 33.82 39.05 | 48.66 50.8 | 49.92 46.89 | 36.11 44.31 | 26.14 30.03 | 40.14 43.2 |
| Augment | * Logit-Adj + COGNISANCE | 43.3 75.13 | 41.19 59.08 | 45.43 27.11 | 42.92 60.7 | 36.01 70.18 | 32.6 52.48 | 36.26 21.76 | 34.51 54.95 |
| | Mixup | 60.14 38.02 | 31.46 56.67 | 7.59 32.82 | 39.35 45.63 | 51.68 32.21 | 23.87 48.25 | 5.47 28.27 | 32.23 38.84 |
| | RandAug | 64.14 42.23 | 40.1 58.27 | 14.96 59.51 | 45.94 52.04 | 55.7 35.87 | 31.61 50.15 | 10.2 47.29 | 38.03 44.01 |
| | * Mixup + COGNISANCE | 67.86 47.9 | 45.5 62.76 | 24.98 67.56 | 51.37 57.54 | 59.28 40.95 | 36.16 54.09 | 17.63 57.72 | 42.63 49.38 |
| Ensemble | * RandAug + COGNISANCE | 69.12 49.31 | 47.64 63.08 | 26.97 67.01 | 53.13 58.16 | 60.85 42.3 | 38.46 55.21 | 19.9 60.11 | 44.63 50.78 |
| | TADE | 57.3 55.22 | 46.85 50.29 | 34.69 37.93 | 49.21 50.41 | 49.61 48.19 | 37.55 42.59 | 27.52 32.21 | 40.87 43.28 |
| | RIDE | 63.18 51.44 | 47.67 52.55 | 29.91 47.38 | 51.21 51.33 | 54.83 44.02 | 38.25 44.2 | 22.77 38.12 | 42.56 43.21 |
| | * TADE + COGNISANCE | 60.69 55.15 | 48.15 52.22 | 33.38 42.12 | 50.95 51.88 | 52.77 48.15 | 39.09 44.06 | 26.51 33.32 | 42.68 44.08 |
| | * RIDE + COGNISANCE | 64.83 54.6 | 50.95 56.21 | 33.28 50.15 | 53.85 54.66 | 57.1 47.63 | 42 48.42 | 25.5 41.23 | 45.57 47.03 |

TABLE II
EVALUATION OF CLT AND GLT PROTOCOLS ON MSCOCO-GLT

| Protocols | | Class-Wise Long Tail (CLT) Protocol | | | | Generalized Long Tail (GLT) Protocol | | | |
|---|--------------------------|-------------------------------------|-----------------------------|----------------------------|-----------------------------|--------------------------------------|-----------------------------|---------------------|-----------------------------|
| $\langle \text{Accuracy} \mid \text{Precision} \rangle$ | | $Many_C$ | $Medium_C$ | Few_C | Overall | $Many_C$ | $Medium_C$ | Few_C | Overall |
| Re-balance | Baseline | 81.27 71.08 | 74.13 76.06 | 50.17 85.61 | 71.88 76.15 | 74.59 64.82 | 66.25 69.08 | 35.75 77.22 | 63.1 69.14 |
| | BBN | 83.59 70.21 | 76.13 76.3 | 47.25 90.98 | 72.98 77.02 | 75.36 61.97 | 68.29 68.61 | 31.75 81.38 | 63.41 68.73 |
| | BLSoftmax | 80.77 71.87 | 75.67 69.94 | 45.25 90.08 | 71.31 74.84 | 73.23 65.13 | 68.63 62.64 | 32.08 79.6 | 62.81 67.09 |
| | Logit-Adj | 81.55 73.95 | 76 75.55 | 60.83 82.04 | 74.97 76.28 | 73.64 66.98 | 68.71 67.61 | 46.58 70.69 | 66 68.01 |
| | GLTv1 | 82.45 73.09 | 76.42 79.53 | 55.58 86.87 | 74.4 78.6 | 76.41 67.07 | 67.33 70.54 | 39.75 81.02 | 65.07 71.39 |
| | * Baseline + COGNISANCE | 83 73.95 | 77.88 80.48 | 55.92 90.08 | 75.28 79.99 | 76.91 68.24 | 67.5 71.41 | 39.67 80.33 | 65.31 72.05 |
| | * BLSoftmax + COGNISANCE | 83 74.17 | 78.37 76.24 | 53.92 86.51 | 75.07 77.58 | 75.86 67.98 | 70.46 68.14 | 40.08 80.26 | 66.22 70.59 |
| Augment | * Logit-Adj + COGNISANCE | 82.68 77.16 | 80.17 75.45 | 59.17 83.54 | 76.78 77.77 | 75.14 70.56 | 71.54 66.34 | 45.83 73.9 | 67.59 69.5 |
| | Mixup | 82.41 72.95 | 73.12 79.53 | 54.33 87.47 | 72.76 78.68 | 74.64 66.43 | 65.33 71 | 36 78.11 | 62.79 70.74 |
| | RandAug | 84.23 74.33 | 77.42 79.28 | 56.33 87.07 | 75.64 79.01 | 77.91 68.56 | 69.67 70.95 | 39.58 78.43 | 66.57 71.59 |
| | * Mixup + COGNISANCE | 85 76.96 | 81.42 83.19 | 63.33 88.89 | 79.03 82.01 | 79.23 70.89 | 72.25 74.84 | 46.5 80.62 | 69.57 74.54 |
| Ensemble | * RandAug + COGNISANCE | 86.55 78.31 | 81.5 82.82 | 62.42 90.29 | 79.47 82.65 | 79.05 69.93 | 72.92 74.51 | 44.33 81.82 | 69.33 74.28 |
| | TADE | 83.55 76.47 | 80.79 73.89 | 50.5 89.34 | 75.57 78.06 | 77.18 68.62 | 71.58 65.63 | 33.5 82.32 | 65.83 70.22 |
| | RIDE | 84.23 77.56 | 82.29 77.79 | 58.42 89.69 | 78.09 80.16 | 77.45 71.2 | 75.17 68.67 | 41.25 83.33 | 69.02 72.66 |
| | * TADE + COGNISANCE | 85.59 77.48 | 82.25 77.85 | 55.08 90.4 | 77.9 80.31 | 79 70.54 | 73.96 68.94 | 40.67 83.65 | 68.98 72.59 |
| | | 86.27 79.64 | 83.13 79.89 | 63.5 90.41 | 80.26 81.98 | 80.09 72.77 | 75.17 71.45 | 47.83 83.03 | 71.38 74.34 |

tailed methods into three categories: 1) Class Re-balancing, 2) Information Augmentation, and 3) Module Improvement, and take two effective methods from each of these three categories for comparison and enhancement, in which we chose two methods, **BLSoftmax** [23] and **Logit-Adj** [6], in the Class Re-balancing category. For Information Augmentation we chose two methods, **Mixup** [34] and **RandAug** [32], and for Module Improvement category we chose two methods, **RIDE** [35] and **TADE** [36], which adopt the idea of ensemble learning and are both current SOTA methods. In addition, we have included the first strong baseline GLTv1 [8] in the GLT domain as a comparison, as shown in Table I and Table II, where the methods with an asterisk are the ones that add our component, and the bolded numbers are the optimal results in the category of the method, and it can be seen that our proposed method gets the best results in all the classifications, especially when combined with the method RandAug or the method RIDE got the best results in almost all evaluation metrics in both datasets.

In addition, this method aims to deal with both intra-class long-tailed and inter-class long-tailed, although the starting point of this method is to solve the problem of attribute long-tailed within the class, but it also meets the challenge of inter-class long-tailed by eliminating the false correlation caused by long-tailed attributes [8]. From Fig. 7, we can see more clearly the improvements that COGNISANCE achieves over the existing LT approaches on the two protocols of the two benchmarks, and we can see that the performance of all the methods from CLT to GLT has been degraded, which also shows that the long-tailed problem is not purely inter-class long-tailed, while intra-class long-tailed is much more challenging, but COGNISANCE can still successfully improve all existing popular LT methods.

Finally, Table III records the experimental results of various

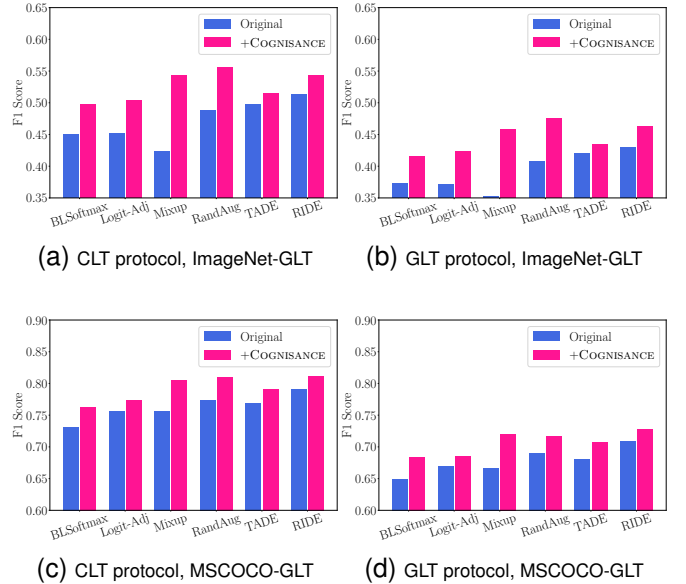


Fig. 7. COGNISANCE enhancements to existing LT methods

methods on the test set of long-tailed distribution, which is consistent with the distribution of the training set, and we can see that compared with other methods, our methods can still achieve the best results on all evaluation metrics.

V. DISCUSSION AND FURTHER ANALYSES

A. Why not directly apply the OLeaF?

In this scheme, CLF is more appropriate compared to OLeaF for two very important characteristics: 1) Automatic tree-splitting mechanism, the number of parameters of CLF is relatively small, and the fine degree of tree-splitting can be

TABLE III
EVALUATION OF IMAGENET-GLT AND MSCOCO-GLT ON LT TEST SET

| Benchmarks | | ImageNet-GLT | | | MSCOCO-GLT | | |
|--------------------|--------------------------|--------------|--------------|--------------|--------------|--------------|--------------|
| Overall Evaluation | | <i>Acc</i> | <i>Prec</i> | <i>F1</i> | <i>Acc</i> | <i>Prec</i> | <i>F1</i> |
| Re-balance | Baseline | 53.93 | 44.46 | 48.74 | 85.74 | 79.98 | 82.76 |
| | BBN | 58.6 | 48.9 | 53.32 | 84.84 | 78.04 | 81.3 |
| | BLSoftmax | 51.73 | 41.97 | 46.34 | 83.69 | 73.81 | 78.44 |
| | Logit-Adj | 50.94 | 40.58 | 45.17 | 85.28 | 73.6 | 79.01 |
| | GLTv1 | 58.28 | 50.43 | 54.07 | 86.67 | 81.88 | 84.21 |
| | * Baseline + COGNISANCE | 58.85 | 50.98 | 54.64 | 86.86 | 81.24 | 83.96 |
| | * BLSoftmax + COGNISANCE | 56.24 | 47.58 | 51.55 | 86.55 | 78.48 | 82.32 |
| | * Logit-Adj + COGNISANCE | 43.61 | 55.15 | 48.71 | 85.52 | 73.36 | 78.98 |
| Augment | Mixup | 55.25 | 46.76 | 50.66 | 86.95 | 82 | 84.4 |
| | RandAug | 59.88 | 51.28 | 55.25 | 87.64 | 81.02 | 84.2 |
| | * Mixup + COGNISANCE | 64.09 | 56.57 | 60.09 | 88.81 | 81.55 | 85.03 |
| | * RandAug + COGNISANCE | 65.15 | 56.85 | 60.72 | 89.12 | 84.02 | 86.49 |
| Ensemble | TADE | 55.21 | 46.52 | 50.49 | 86.57 | 79.91 | 83.1 |
| | RIDE | 60.17 | 48.28 | 53.58 | 88.03 | 81.79 | 84.8 |
| | * TADE + COGNISANCE | 58.06 | 47.44 | 52.21 | 88 | 81.72 | 84.74 |
| | * RIDE + COGNISANCE | 62.11 | 50.8 | 55.89 | 89.02 | 81.85 | 85.28 |

controlled only by adjusting the parameter d_{max} . The tree-splitting scheme in OLeaF is more rigorous and detailed but requires a certain degree of manual analysis, whereas the feature learner needs to be iterated in this framework, and it may be possible after each iteration to re-trigger clustering, and the dataset targeted is often large image data, so a fully automated scheme must be needed; 2) CoarseNode, each node of CLF is a coarse-grained node, the reason why this mechanism is designed mainly to deal with the long-tailed problem of attributes within a category, due to the fact that the head attribute may contain a large number of similar samples, and if left uncontrolled, the length of the path occupied by the head attribute may skyrocket, while each node in the same path is sampled with the same weight, a large number of extremely similar nodes actually lose their representativeness, and at the same time, the sampling weights of bottom nodes are compromised, so it is necessary to carry out a small range of clustering to be controlled, and this clustering process is mainly controlled by the parameter d_{min} , and all the members of the nodes within a CoarseNode will equally share the node's sampling weight.

B. Why not directly apply IRM loss?

In this scheme, there are two reasons why IRM loss is not used directly: 1) the original IRM loss has convergence problems on real-world large-scale image datasets; 2) the core in Multi-Center Loss lies in the Multi-center, which is a mechanism that can make the model's learning more robust because the samples within the same category in an artificial dataset may gap tremendously, and at this time, if we simply add the regularity of one center, it will instead impair the learning of the features.

C. About Parameter Adjustment

In this scheme, there are two types of parameters that can be tuned: 1) overall process-related, e.g., the number of epochs

for warm-up, the number of epoch steps for updating the sampling weights of samples, and the number of environments; and 2) clustering-related, the two parameters d_{min} and d_{max} in CLF clustering, the former controlling the radius of the CoarseNode and the latter controls the fineness of the tree splitting. The algorithm is preset with two relatively general default values, but they can still be adjusted according to the specific dataset. The above parameters have little impact on the overall effect within a certain range, but there is still room for further optimization.

D. About Distance Measure

In this scheme, the distance metric is used in two places: 1) CLF construction, the distance matrix needs to be calculated when CLF clustering is carried out, and the distance metric here can be switched arbitrarily; 2) Multi-Center Loss, the distance from the samples to the center of their belonging will be calculated when optimizing the MCL, and the distance metric here is consistent with that of CLF construction, and it can also be switched freely. The Euclidean distance is used as the default distance metric in this paper, switching other metrics may give better results, due to the relatively large amount of work, only one metric is used here, but it does not affect the elaboration of the main idea.

E. About Eliminating Noise

Any real-world dataset is imperfect, and noisy samples such as sensory glitches (e.g., low-quality or corrupted images) and human errors (e.g., mislabeling or ambiguous annotations) may impair model training. In this scheme, the proposed CLF actually has the potential to perform noise identification, as shown in Fig. 4, if there is a tree in the CLF contains only one node and the node contains only one sample, or the node is a leaf node of a very deep tree, then the sample corresponding to this node have a high probability of being noise samples,

which can be further processed to finalize whether they are noise or not, and this idea can be explored more in future work.

VI. CONCLUSION

In this study, we provide insights into the long-tailed problem at two levels of granularity: inter-class and intra-class, and propose two important components: the CLF (Coarse-Grained Leading Forest) and the MCL (Multi-Center Loss). The CLF, as an unsupervised learning methodology, aims to capture the distribution of attributes within a class in order to lead the construction of multiple environments, thus supporting the invariant feature learning. Meanwhile, MCL, as an evolutionary version of Center Loss, aims to replace the traditional IRM Loss to further enhance the robustness of the model on real-world datasets.

Through extensive experiments on existing benchmarks MSCOCO-GLT and ImageNet-GLT, we exhaustively demonstrate the significant results of our method. Finally, we would also like to point out the advantages of the two components, CLF and MCL, which are designed as low-coupling plugins that can be organically integrated with other long-tailed classification methods, bringing new possibilities for model performance improvement.

ACKNOWLEDGMENT

This work has been supported by the National Natural Science Foundation of China under grants 61966005, 61936001 and 62366008, the National Key Research and Development Program of China under grant 2020YFB1713300, the Natural Science Foundation of Chongqing (cstc2019jcyjcxxtX0002, cstc2021ycjh-bgzxm0013), and the Key Collaboration Project of Chongqing Municipal Education Commission(HZ2021008).

REFERENCES

- [1] Y. Zhang, B. Kang, B. Hooi, S. Yan, and J. Feng, "Deep long-tailed learning: A survey," *IEEE Transactions on Pattern Analysis and Machine Intelligence*, 2023.
- [2] Y. Yang, H. Wang, and D. Katabi, "On multi-domain long-tailed recognition, imbalanced domain generalization and beyond," in *European Conference on Computer Vision*, pp. 57–75, Springer, 2022.
- [3] M. Buda, A. Maki, and M. A. Mazurowski, "A systematic study of the class imbalance problem in convolutional neural networks," *Neural networks*, vol. 106, pp. 249–259, 2018.
- [4] S. Ando and C. Y. Huang, "Deep over-sampling framework for classifying imbalanced data," in *Machine Learning and Knowledge Discovery in Databases: European Conference, ECML PKDD 2017, Skopje, Macedonia, September 18–22, 2017, Proceedings, Part I 10*, pp. 770–785, Springer, 2017.
- [5] Y. Yang, G. Zhang, D. Katabi, and Z. Xu, "Me-net: Towards effective adversarial robustness with matrix estimation," *arXiv preprint arXiv:1905.11971*, 2019.
- [6] K. Cao, C. Wei, A. Gaidon, N. Arechiga, and T. Ma, "Learning imbalanced datasets with label-distribution-aware margin loss," *Advances in neural information processing systems*, vol. 32, 2019.
- [7] L. Sun, K. Wang, K. Yang, and K. Xiang, "See clearer at night: towards robust nighttime semantic segmentation through day-night image conversion," in *Artificial Intelligence and Machine Learning in Defense Applications*, vol. 11169, pp. 77–89, SPIE, 2019.
- [8] K. Tang, M. Tao, J. Qi, Z. Liu, and H. Zhang, "Invariant feature learning for generalized long-tailed classification," in *European Conference on Computer Vision*, pp. 709–726, Springer, 2022.
- [9] C. Drummond, R. C. Holte, *et al.*, "C4. 5, class imbalance, and cost sensitivity: why under-sampling beats over-sampling," in *Workshop on learning from imbalanced datasets II*, vol. 11, pp. 1–8, 2003.
- [10] H. Han, W.-Y. Wang, and B.-H. Mao, "Borderline-smote: a new over-sampling method in imbalanced data sets learning," in *International conference on intelligent computing*, pp. 878–887, Springer, 2005.
- [11] H. He and E. A. Garcia, "Learning from imbalanced data," *IEEE Transactions on knowledge and data engineering*, vol. 21, no. 9, pp. 1263–1284, 2009.
- [12] T.-Y. Lin, P. Goyal, R. Girshick, K. He, and P. Dollár, "Focal loss for dense object detection," in *Proceedings of the IEEE international conference on computer vision*, pp. 2980–2988, 2017.
- [13] B. Kang, S. Xie, M. Rohrbach, Z. Yan, A. Gordo, J. Feng, and Y. Kalantidis, "Decoupling representation and classifier for long-tailed recognition," in *International Conference on Learning Representations*, 2019.
- [14] B. Zhou, Q. Cui, X.-S. Wei, and Z.-M. Chen, "Bbn: Bilateral-branch network with cumulative learning for long-tailed visual recognition," in *Proceedings of the IEEE/CVF conference on computer vision and pattern recognition*, pp. 9719–9728, 2020.
- [15] B. Zhu, Y. Niu, X.-S. Hua, and H. Zhang, "Cross-domain empirical risk minimization for unbiased long-tailed classification," in *Proceedings of the AAAI Conference on Artificial Intelligence*, vol. 36, pp. 3589–3597, 2022.
- [16] P. Cui and S. Athey, "Stable learning establishes some common ground between causal inference and machine learning," *Nature Machine Intelligence*, vol. 4, no. 2, pp. 110–115, 2022.
- [17] M. Arjovsky, L. Bottou, I. Gulrajani, and D. Lopez-Paz, "Invariant risk minimization," *stat*, vol. 1050, p. 27, 2020.
- [18] E. Creager, J.-H. Jacobsen, and R. Zemel, "Environment inference for invariant learning," in *International Conference on Machine Learning*, pp. 2189–2200, PMLR, 2021.
- [19] Y. Wen, K. Zhang, Z. Li, and Y. Qiao, "A discriminative feature learning approach for deep face recognition," in *Computer Vision—ECCV 2016: 14th European Conference, Amsterdam, The Netherlands, October 11–14, 2016, Proceedings, Part VII 14*, pp. 499–515, Springer, 2016.
- [20] T. Wang, Y. Li, B. Kang, J. Li, J. Liew, S. Tang, S. Hoi, and J. Feng, "The devil is in classification: A simple framework for long-tail instance segmentation," in *Computer Vision—ECCV 2020: 16th European Conference, Glasgow, UK, August 23–28, 2020, Proceedings, Part XIV 16*, pp. 728–744, Springer, 2020.
- [21] A. Estabrooks, T. Jo, and N. Japkowicz, "A multiple resampling method for learning from imbalanced data sets," *Computational intelligence*, vol. 20, no. 1, pp. 18–36, 2004.
- [22] Z. Zhang and T. Pfister, "Learning fast sample re-weighting without reward data," in *Proceedings of the IEEE/CVF International Conference on Computer Vision*, pp. 725–734, 2021.
- [23] J. Ren, C. Yu, X. Ma, H. Zhao, S. Yi, *et al.*, "Balanced meta-softmax for long-tailed visual recognition," *Advances in neural information processing systems*, vol. 33, pp. 4175–4186, 2020.
- [24] C. Elkan, "The foundations of cost-sensitive learning," in *International joint conference on artificial intelligence*, vol. 17, pp. 973–978, Lawrence Erlbaum Associates Ltd, 2001.
- [25] M. A. Jamal, M. Brown, M.-H. Yang, L. Wang, and B. Gong, "Re-thinking class-balanced methods for long-tailed visual recognition from a domain adaptation perspective," in *Proceedings of the IEEE/CVF Conference on Computer Vision and Pattern Recognition*, pp. 7610–7619, 2020.
- [26] J. Tan, C. Wang, B. Li, Q. Li, W. Ouyang, C. Yin, and J. Yan, "Equalization loss for long-tailed object recognition," in *Proceedings of the IEEE/CVF conference on computer vision and pattern recognition*, pp. 11662–11671, 2020.
- [27] J. Tan, X. Lu, G. Zhang, C. Yin, and Q. Li, "Equalization loss v2: A new gradient balance approach for long-tailed object detection," in *Proceedings of the IEEE/CVF conference on computer vision and pattern recognition*, pp. 1685–1694, 2021.
- [28] A. K. Menon, S. Jayasumana, A. S. Rawat, H. Jain, A. Veit, and S. Kumar, "Long-tail learning via logit adjustment," *arXiv preprint arXiv:2007.07314*, 2020.
- [29] P. Chu, X. Bian, S. Liu, and H. Ling, "Feature space augmentation for long-tailed data," in *Computer Vision—ECCV 2020: 16th European Conference, Glasgow, UK, August 23–28, 2020, Proceedings, Part XXIX 16*, pp. 694–710, Springer, 2020.
- [30] J. Wang, T. Lukasiewicz, X. Hu, J. Cai, and Z. Xu, "Rsg: A simple but effective module for learning imbalanced datasets," in *Proceedings of the IEEE/CVF Conference on Computer Vision and Pattern Recognition*, pp. 3784–3793, 2021.

- [31] X. Hu, Y. Jiang, K. Tang, J. Chen, C. Miao, and H. Zhang, "Learning to segment the tail," in *Proceedings of the IEEE/CVF conference on computer vision and pattern recognition*, pp. 14045–14054, 2020.
- [32] E. D. Cubuk, B. Zoph, J. Shlens, and Q. V. Le, "Randaugment: Practical automated data augmentation with a reduced search space," in *Proceedings of the IEEE/CVF conference on computer vision and pattern recognition workshops*, pp. 702–703, 2020.
- [33] J. Liu, Y. Sun, C. Han, Z. Dou, and W. Li, "Deep representation learning on long-tailed data: A learnable embedding augmentation perspective," in *Proceedings of the IEEE/CVF conference on computer vision and pattern recognition*, pp. 2970–2979, 2020.
- [34] H. Zhang, M. Cisse, Y. N. Dauphin, and D. Lopez-Paz, "mixup: Beyond empirical risk minimization," *arXiv preprint arXiv:1710.09412*, 2017.
- [35] X. Wang, L. Lian, Z. Miao, Z. Liu, and S. Yu, "Long-tailed recognition by routing diverse distribution-aware experts," in *International Conference on Learning Representations*, 2020.
- [36] Y. Zhang, B. Hooi, L. Hong, and J. Feng, "Self-supervised aggregation of diverse experts for test-agnostic long-tailed recognition," *Advances in Neural Information Processing Systems*, vol. 35, pp. 34077–34090, 2022.
- [37] J. Xu, G. Wang, and W. Deng, "Denpehc: Density peak based efficient hierarchical clustering," *Information Sciences*, vol. 373, pp. 200–218, 2016.
- [38] A. Rodriguez and A. Laio, "Clustering by fast search and find of density peaks," *science*, vol. 344, no. 6191, pp. 1492–1496, 2014.
- [39] O. Russakovsky, J. Deng, H. Su, J. Krause, S. Satheesh, S. Ma, Z. Huang, A. Karpathy, A. Khosla, M. Bernstein, *et al.*, "Imagenet large scale visual recognition challenge," *International journal of computer vision*, vol. 115, pp. 211–252, 2015.
- [40] G. Patterson and J. Hays, "Coco attributes: Attributes for people, animals, and objects," in *Computer Vision—ECCV 2016: 14th European Conference, Amsterdam, The Netherlands, October 11–14, 2016, Proceedings, Part VI 14*, pp. 85–100, Springer, 2016.



JinYE Yang received the B.E degree from Yanshan University, Qinhuangdao, China in 2019. He is currently a graduate student with the State Key Laboratory of Public Big Data, Guizhou University. His current research interests include granular computing and machine learning.



Ji Xu received the B.S. from Beijing Jiaotong University in 2004 and the Ph.D. from Southwest Jiaotong University, Chengdu, China, in 2017, respectively. Both degrees are in the major of Computer Science. Now he is an associate professor with the State Key Laboratory of Public Big Data, Guizhou University. His research interests include data mining, granular computing and machine learning. He has authored and co-authored over 10 papers in refereed international journals such as IEEE TCYB, Information Sciences, Knowledge-Based Systems

and Neurocomputing.